Infinite Dilution Activity Coefficients and Miscibility Using a Modified Static Total Pressure Method

Julie N. Howat and Colin S. Howat*

Kurata Thermodynamics Laboratory, Department of Chemical & Petroleum Engineering, University of Kansas, Lawrence, Kansas 66045-2223

This paper presents a modified static total pressure method coupled with appropriate data analysis procedures which provide infinite dilution activity coefficients (γ^{∞}) and solubility (x^{sat}) for volatile organic compounds in water. A large, calibrated vapor space minimizes the impact of noncondensable compounds. The degassed solute is micrometered incrementally into the cell containing water. The meterings continue into the two-liquid-phase region. This results in a discontinuous P,z curve. The number of measurements taken for each experimental composition are greater than the number required to establish equilibrium. Data reconciliation methods accounting for the errors allow use of all measurements to provide estimates of γ^{∞} and x^{sat}. Experimental design methods testing the impact of experimental errors, potential sources of bias, and the number and volume of the solute meterings verify the accuracy and precision of the resultant γ^{∞} and x^{sat} values. Experimental results for acetone + water and experimental design studies of partially miscible systems are presented.

Introduction

Health and environmental considerations require removal of harmful volatile organic chemicals (VOC's) from wastewater and polymers for indoor use. The phase equilibria in a typical VOC removal process for rejection of VOC from latex polymer is complex. The phases include a water-rich liquid phase, a VOC-rich liquid phase, an adsorbed organic phase, and a vapor phase. The polymer is essentially nonvolatile. In addition, there is the potential for an occluded liquid phase comprised of an organic, water, or both phases. The organic solvent must be removed to very low levels (ppm or ppb) in the polymer product. Design requires a description of this phase and material balance behavior. Reliable data and descriptions thereof, particularly in the infinitely dilute region, are typically unavailable. Hartwick and Howat (1993) showed that extrapolation of full-range composition VOC + water data into the infinite dilution region introduces systematic error in the estimated phase equilibria and subsequent process design.

This paper extends the developments of Hartwick and Howat (1995) into those VOC + water systems exhibiting limited miscibility such that γ^{∞} and x^{sat} are measured for sparingly-soluble VOC's in water. The reconciliation methods of MacDonald and Howat (1988) and Kuo (1988) are tested to account for all experimental measurements in the data analysis. Figure 1 shows a typical total pressure curve for a binary VOC + water system. The discontinuity in the pressure−bulk composition curve marks the transition between the dilute liquid−vapor boundary, where the pressure rises as the bulk liquid mole fraction of VOC increases, and the liquid−liquid−vapor boundary, where the pressure remains constant. The discontinuity occurs at x^{sat}. Depending upon the value of x^{sat}, the VOC nonideality and the precision and accuracy of the experimental equipment, three regions in the x,γ^{∞} space can be defined:

Region 1: There is sufficient x space below x^{sat} to allow proper extrapolation of the P,x curve to infinite dilution. This extrapolation is described by Hartwick and Howat (1995) to estimate γ^{∞}. x^{sat} is estimated from the calculated liquid composition at the discontinuity in the P,x curve. Because a vapor−liquid−liquid flash is not calculated, no solution model dependence is introduced in the estimation of x^{sat}.

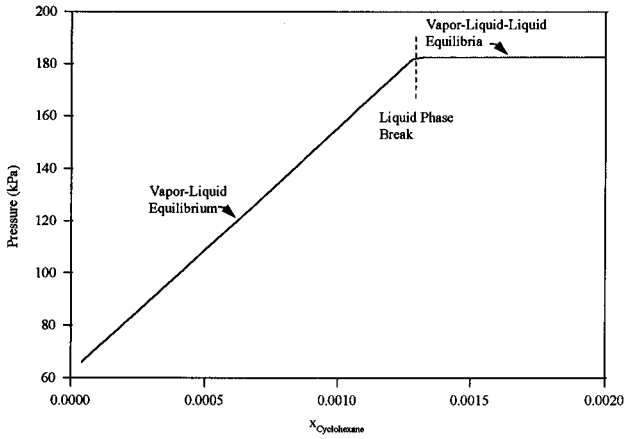

Figure 1. Total pressure versus liquid composition for cyclohexane−water at 360 K (UNIQUAC equation).

Region 2: There is insufficient x space below x^{sat} to allow proper extrapolation of the P,x curve to infinite dilution, but sufficient space to measure some pressures in the vapor−liquid region. The solution model must now be called upon to describe both the vapor−liquid and the vapor−liquid−liquid equilibria. Region 2 data analysis contains more solution model dependence than does Region 1.

Region 3: There is insufficient x space below x^{sat} to allow any reliable metering of pure VOC. The P,x curve is generated by incrementally metering VOC-saturated water. Region 3 data analysis relies completely on the ability of the solution model to simultaneously describe γ^{∞} and x^{sat}. It is important to recognize that the boundaries of the regions are functions of the experimental measurement errors as well as the values of γ^{∞} and x^{sat}.

Theoretical Development−Estimation of γ_1^{∞}

Hartwick and Howat (1995) based their γ_1^{∞} calculation on the equation developed by Gautreaux and Coates (1955)

* To whom correspondence should be addressed. howat@cpe.engr.ukans.edu.

S0021-9568(96)00026-X CCC: $12.00

which relates the infinite dilution activity coefficient to the partial derivative of pressure with respect to liquid composition.

$$\gamma_1^\infty = (P/P_1^\circ)(1 + (1/P)(\partial P/\partial x_1)_T^{x=0}) \quad (1)$$

where P is the total pressure, P_1° is the vapor pressure of the VOC, x_1 is the VOC liquid mole fraction, and T is the temperature. Equation 1 is valid for ideal vapor behavior and where the vapor volume is much greater than the liquid volume ($V^V \gg V^L$). It is possible to develop a similar expression which is not subject to these restrictions. Gautreaux and Coates (1955) include one such development. A simpler development follows.

Begin with a rigorous expression for total pressure:

$$P = \gamma_1 x_1 \phi_1^\circ P_1^\circ \mathrm{PC}_1/\hat{\phi}_1 + \gamma_2 x_2 \phi_2^\circ P_2^\circ \mathrm{PC}_2/\hat{\phi}_2 \quad (2)$$

where γ_i is the activity coefficient of component i, ϕ_i° and $\hat{\phi}_i$ are the fugacity coefficients of component i in pure i and in the mixture, respectively, and PC_i is the Pointing correction given as eq 3.

$$\mathrm{PC}_i = \exp\left[\int_{P_i^\circ}^{P} V_i^L/RT \, dP\right] \quad (3)$$

Grouping the vapor nonidealities into a single term:

$$\Phi_i = (\phi_i^\circ/\hat{\phi}_i)\mathrm{PC}_i \quad (4)$$

Combine eqs 2 and 3, solve for γ_1, and take the limit as $x_1 \rightarrow 0$:

$$\gamma_1^\infty = \lim_{x_1 \rightarrow 0}\{(P - \gamma_2 x_2 P_2^\circ \Phi_2)/x_1 P_1^\circ \Phi_1)\} \quad (5)$$

Equation 5 must be evaluated using l'Hôpital's rule:

$$\gamma_1^\infty = \lim_{x_1 \rightarrow 0}\left\{\frac{\partial}{\partial x}(P - \gamma_2 x_2 P_2^\circ \Phi_2)/\frac{\partial}{\partial x}(x_1 P_1^\circ \Phi_1)\right\} \quad (6)$$

The remainder of the development consists of taking the derivatives and evaluating the resulting expressions in the limit. The following expression is useful in evaluating the fugacity coefficient derivative (Walas, 1985, p 142):

$$(1/\hat{\phi}_i)\partial\hat{\phi}_i/\partial x_1 = \partial \ln \hat{\phi}_i/\partial x_1 = (\partial P/\partial x_1)(\partial \ln \hat{\phi}_i/\partial P) = (\partial P/\partial x_1)\{(\bar{V}_2 - \bar{V}_2^{id})/RT\} \quad (7)$$

In the limit, the following expressions apply:

$$x_2 \rightarrow 1$$

$$\gamma_2 \rightarrow 1$$

$$P \rightarrow P_2^\circ \quad (8)$$

$$\hat{\phi}_2 \rightarrow \hat{\phi}_2^\circ$$

$$\mathrm{PC}_2 \rightarrow 1$$

$$\partial\gamma_2/\partial x_1 \rightarrow 0$$

The resulting expression is equivalent to the expression given by Maher and Smith (1979):

$$\gamma_1^\infty = (\hat{\phi}_1 P_2^\circ/\phi_1^\circ P_1^\circ)[1 + (\partial P/\partial x_1)_{x_1=0}\{(V_2^V - V_2^L)/RT\}] \exp\int_{P_2^\circ}^{P_1^\circ} V_1^L/RT \, dP \quad (9)$$

All terms but the limiting slope of the pressure versus liquid composition curve can be calculated from pure component properties. $(\partial P/\partial x_1)_{x_1=0}$ must be estimated from pressure versus composition data. The most direct approach to estimating the derivative is to extrapolate P,x data to $x_1 = 0$ and then calculate the slope at that point. Maher and Smith (1979) state that it is difficult to fit a curve to the P,x data which can support reliable calculation of the slope at $x_1 = 0$. Hartwick and Howat (1995) used the method of Ellis and Jonah (1962) to estimate the derivative.

$$P_D = P - x_1 P_1^\circ - x_2 P_2^\circ = P - \{P_2^\circ + (P_1^\circ - P_2^\circ)x_1\} \quad (10)$$

$$\partial P/\partial x_1 = \partial P_D/\partial x_1 + P_1^\circ - P_2^\circ \quad (11)$$

The limit as $x_1 \rightarrow 0$ of P_D/x_1x_2 by l'Hôpital's rule is the derivative with respect to x_1 of P_D:

$$\lim_{x_1 \rightarrow 0}(P_D/x_1x_2) = \lim_{x_1 \rightarrow 0}\{(\partial P_D/\partial x_1)/(1 - 2x_1)\} = (\partial P_D/\partial x_1)_{x_1=0} \quad (12)$$

2 Extrapolation of P_D/x_1x_2 to $x_1 = 0$ allows estimation of $(\partial P/\partial x_1)_{x_1=0}$ without calculating the slope of the extrapolated curve.

$$(\partial P/\partial x_1)_{x_1=0} = \lim_{x_1 \rightarrow 0}(P_D/x_1x_2) + P_1^\circ - P_2^\circ \quad (13)$$

Maher and Smith (1979) state that, depending on the system, either P_D/x_1x_2 or its inverse is frequently linear, allowing reliable extrapolation of P,x data.

Two points should be emphasized from the discussion above. First, both eqs 9 and 13 are rigorous and contain no dependence upon the liquid solution model. Second, the reliability of the estimation of γ_1^∞ from P,x data depends upon the accuracy and precision of the P,x data and the reliability of the extrapolation of P_D/x_1x_2 or its inverse to $x_1 = 0$.

Theoretical Development—Coupled γ_1^∞ and x_1^{sat}

The saturation limit of the VOC in water, x_1^{sat}, imposes an upper limit on the compositions for which the required P,x data can be measured. The experimental design calculations described below address this complication for region 1 systems.

For region 2 and 3 systems, an additional concern is increasing dependence upon the solution model during data analysis. Whereas in region 1 systems, the solution model is used only to calculate x from the bulk mole fraction, z, via liquid−vapor flash, in region 2 systems, it must also be used to calculate x_1^{sat} and in region 3 systems, z also depends on x_1^{sat}. The effect of this increasing solution model dependence may be to introduce bias into the resultant estimates. It is mitigated by the limiting relationship between γ^∞ and x^{sat}.

For liquid−liquid equilibrium:

$$\gamma_1 x_1 = \gamma_1^* x_1^* \quad (14)$$

where the superscript * represents a second liquid phase. If there is very little water in the organic phase, then

$$\gamma_1 x_1 \approx 1 \quad (15)$$

and

$$\lim_{x_1^{sat} \rightarrow 0}(x_1^{sat}) = 1/\gamma_1^\infty \quad (16)$$

Systems with extremely high γ_1^∞'s and extremely low x_1^{sat}'s must approach this limit regardless of the solution model used. Figure 2 shows the relation between γ_1^∞ and x_1^{sat} as a function of the solution model. As γ_1^∞ increases, potential solution model bias decreases.

Data Reconciliation

In Hartwick and Howat's (1995) data analysis method, the flash required to calculate x from z is overspecified. In the experimental method, five variables are measured:

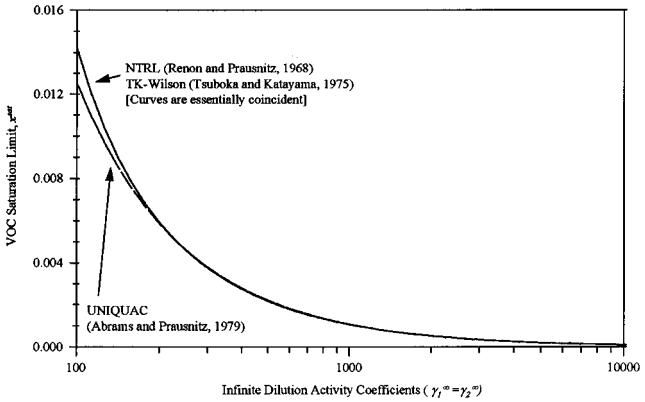

Figure 2. Sensitivity of calculated x^{sat} to solution model.

pressure, temperature, total volume, and metered moles of the VOC and water (P, T, V_{total}, F_1, and F_2). Four parameters are unknown: the moles of each component in the liquid and vapor phases (L_1, L_2, V_1, and V_2). There are five constraints: two material balances, two equilibrium constraints, and one total volume constraint. The flash calculation used in the data analysis is subject to these five constraints and must generate five unknown parameters. With only four truly unknown parameters available, a fifth must be selected from among the measured variables. They chose to select P as the fifth parameter. Thus, their flash calculation, and consequently their liquid phase mole fractions, were based on the measured T, V_{total}, F_1, and F_2. The measured P information was effectively discarded. In addition, they had a possible sixth measured variable, the liquid volume in the cell (V_{liquid}). Had they measured this, as well, they would have had to ignore two experimental measurements.

A substitute for the flash which includes all measured variables has been developed for this work. It is based on the constrained maximum likelihood estimation used in the plant performance analysis developments of MacDonald and Howat (1988) and Kuo (1988). It uses all six—or in the case of Hartwick and Howat, five—experimental variables. These variables are adjusted to minimize the error between their measured and adjusted values while conforming to the flash constraints. This alternative accounts properly for all experimental errors, uses all experimental measurements, and closes the material balance and equilibrium constraints. Potential drawbacks include the markedly increased complexity and time required for the reconciled flash calculation and the increased solution model dependence introduced by the constraints.

In the discussion below, the *variables* are the experimental measurements and the *parameters* are the unknown liquid and vapor moles. The *constraints* are the material balances, the equilibrium relations, the total volume, and the liquid volume. Lagrange multipliers are used to impose the constraints on the maximum likelihood estimation. This development is based upon the work of MacDonald and Howat (1988) without the limitations of the linearization of Britt and Luecke (1973) imposed.

Mathematically,

Minimize

$$S = (1/2)\Delta\vec{Z}^{T}\mathbf{J}^{-1}\Delta\vec{Z} \tag{17}$$

Subject to

$$\vec{f}(\vec{Z},\vec{\theta}) = 0 \tag{18}$$

where $\Delta\vec{Z}$ is the vector of the difference between the measured and adjusted variables, $\mathbf{J}^{-1}$ is the inverse of the variance—covariance matrix of the experimental measurements, $\vec{f}$ is the vector of constraints, and $\vec{\theta}$ is the vector of parameters.

Specifically,

$$\Delta\vec{Z} = \vec{Z}^{m} - \vec{Z} \tag{19}$$

$$\vec{Z} = \begin{bmatrix} T \\ P \\ F_1 \\ F_2 \\ V_{total} \\ V_{liquid} \end{bmatrix} \tag{20}$$

$$\vec{\theta} = \begin{bmatrix} L_1 \\ L_2 \\ V_1 \\ V_2 \end{bmatrix} \tag{21}$$

$$\vec{f}(\vec{Z},\vec{\theta}) = \begin{bmatrix} F_1 - L_1 - V_1 \\ F_2 - L_2 - V_2 \\ V_1/(V_1+V_2) - (\gamma_1 P_1^{sat}/P)(L_1/(L_1+L_2)) \\ V_2/(V_1+V_2) - (\gamma_2 P_2^{sat}/P)(L_2/(L_1+L_2)) \\ V_{total} - V_{liquid} - (V_1+V_2)RT/P \\ V_{liquid} - v_1 L_1 - v_2 L_2 \end{bmatrix} \tag{22}$$

Lagrange multipliers are used to combine S and $\vec{f}$ to give Q.

$$Q(\Delta\vec{Z},\vec{\theta},\vec{\lambda}) = (1/2)\Delta\vec{Z}^{T}\mathbf{J}^{-1}\Delta\vec{Z} + \vec{\lambda}^{T}f(\vec{Z},\vec{\theta}) \tag{23}$$

$Q(\Delta\vec{Z},\vec{\theta},\vec{\lambda})$ is minimized when

$$\mathbf{Q}_z = 0$$

$$\mathbf{Q}_\theta = 0 \tag{24}$$

$$\mathbf{Q}_\lambda = 0$$

The reconciliation procedure gives the variance—covariance matrix for the parameters (Britt and Luecke, 1973):

$$E\{(\vec{\theta} - \vec{\theta}_o)(\vec{\theta} - \vec{\theta}_o)^{T}\} = (\mathbf{F}_\theta^{T}(\mathbf{F}_z\mathbf{J}\mathbf{F}_z^{T})^{-1}\mathbf{F}_\theta\}^{-1} \tag{25}$$

where $\mathbf{F}_\theta$ and $\mathbf{F}_z$ are matrices of derivatives of the constraints with respect to the parameters and variables, respectively. Note that the reconciliation procedure generates covariances among the parameters, even when the covariances among the variables are zero.

This reconciliation of the experimental measurements to the constraints subject to the experimental errors now accounts for all experimental measurements in the estimation of vapor and liquid compositions. The entire result, including reconciled pressure, temperature, and liquid moles can be applied to each experimental point to generate the P,x relation required for the estimation of γ_1^∞. Alternatively, the reconciled liquid moles can be used to generate the x values, but the measured values are retained for temperature and pressure. Note that in applying the above method to the data of Hartwick (1996), the last two constraints of eq 22 are combined. $\vec{Z}$ of eq 20 is reduced to five variables with V_{liquid} eliminated from consideration.

Regression Analysis

For region 1 data analysis, the $P_D/x_1x_2,x_1$ points are fit via weighted linear regression to a first- or second-order polynomial. The curve is extrapolated to provide an estimate for γ_1^∞, i.e. γ_1^∞(extp). Because the solution model parameters, and consequently x_1, depend on γ_1^∞, the pro-

cedure is iterative, continuing until

$$\gamma_1^{\infty}(\text{extp}) = \gamma_1^{\infty} \tag{26}$$

For region 2 data analysis, the same linear regression is used, but the iteration continues until the following objective function is minimized:

$$f = \{[\gamma_1^{\infty}(\text{extp}) - \gamma_1^{\infty}]/\sigma_\gamma\}^2 + \{[x_1^{\text{sat}}(\text{mod}) - x_1^{\text{sat}}(\text{int})]/\sigma_x\}^2 \tag{27}$$

x_1^{sat}(mod) is calculated from the solution model prediction for liquid−liquid equilibrium and x_1^{sat}(int) is calculated using the $P_D/x_1x_2,x_1$ description evaluated at the measured liquid−liquid−vapor pressure.

For region 3 data analysis, eq 27 is again used, but because z is now a function of x_1^{sat}(mod), it must be recalculated at every iteration.

Experimental Section

Hartwick and Howat (1995) review the various experimental methods used to estimate γ_1^{∞}. They conclude that the static total pressure method is the most appropriate for the systems to be studied. They described their experimental equipment and method. It is based on a modified, isothermal, total-pressure method. They maintained a large vapor space in their test cell to minimize the impact of noncondensible contaminants on the measurements. The VOC was micrometered into a fixed volume cell containing a known amount of water. After equilibrium at the desired temperature was established, the pressure was measured. Then, additional VOC was metered, equilibrium was re-established, and pressure was re-measured. Pressure was measured with a Paroscientific Model A100 transducer connected directly to the test cell. Their reported temperature and pressure errors are 0.02 K and 0.1 kPa. The water metering error is 0.15%. VOC metering error depends on the amount metered. For VOC mole fractions above 0.001, the error decreases from 1% to 0.5%, as metered volume increases. For mole fractions below 0.001, metering error increases rapidly as metered volume decreases.

Conclusions from experimental design analysis (Natarajan, 1995) and confirmed in a subsequent section of this paper along with analysis of more data than those included in Hartwick and Howat (1995) show that pressure error is the most significant contributor to the total error in the γ_1^{∞} estimate. Consequently, the equipment was modified to reduce the error in measured pressure to 0.02 kPa.

Figure 3 presents a schematic of the equipment now used for this experimental program. Cell 6 is the test cell in which all total pressure measurements are made. Cells 3 and 4 are variable-volume metering cells used for metering solvent (water, in this case) into cell 6. Cell 5 is the micrometering cell used for metering solute (VOC) into cell 6. Cell 2 is used for metering water saturated with VOC. Cell 1 is idle.

In the pressure measurement method used by Hartwick and Howat (1995), the transducer was connected directly to the test cell. Two potential biases arose. First, the transducer is very sensitive to liquid droplets in the diaphragm connected to the oscillating quartz crystal. Without knowing whether liquid is present, the calibration is uncertain and potentially biased. To guard against this, the transducer was kept under separate temperature control at a temperature slightly above the bath temperature. Temperatures were near the upper limit of the transducer operation. While the calibration of the transducer had been done at various temperatures, the calibration is nonlinear in temperature at the conditions required to minimize the potential for liquid droplets. Imperfect temperature control resulted in imperfect knowledge of the calibration. Consequently, the error in measured pressure was likely to be higher than the calibration error.

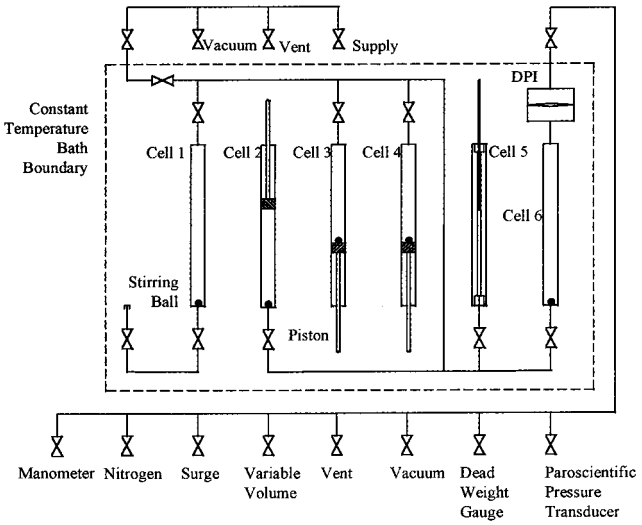

Figure 3. Schematic of experimental equipment.

The transducer is now separated from cell 6 using a diaphragm-linear differential transformer system similar to that used by Laurance and Swift (1974) and Howat (1975). The nonsystem side of the diaphragm is connected to a nitrogen system. Pressure is measured by overpressuring the nitrogen side of the diaphragm and gradually lowering it until null is reached across the diaphragm, as indicated with the linear differential transformer. The pressure is then read directly from the transducer.

Region 1 Experimental Design Results

Hartwick and Howat (1995) concluded from a series of Monte Carlo Simulation-based experimental design calculations for a simulated acetone + water system that

1. A first-order linear fit of P_D/x_1x_2 extrapolated to $x_1 = 0$ to estimate $\partial P/\partial x_1)_{x_1=0}$ was the best method for estimating γ_1^{∞} for the acetone−water system.

2. The optimum range for data acquisition was between $x_1 = 0.001$ and $x_1 = 0.02$. Data acquired below this range were uncertain in pressure relative to P_2° which resulted in a high random error in γ_1^{∞}. Data acquired above this region introduced significant nonlinearity into the P_D/x_1x_2 curve and resulted in increased bias in the estimate for γ_1^{∞}.

3. Data acquired in groups of four compositions, replicated, resulted in superior estimates for γ_1^{∞}. Additional compositions at the expense of replicating data sets did not improve the estimates.

4. Neither the solution model used in the flash calculation nor the estimate for γ_2^{∞} added bias to the estimate for γ_1^{∞}.

To further refine the procedure for region 1, additional experimental design analyses have been conducted. Five principal questions have been addressed. Table 1 presents the results. Each test is the result of analyses of 1000 artificial data sets generated by adding random experimental error to a canonical data set. The bias of the average calculated γ_1^{∞} indicates the accuracy resulting from the parameters of the test. The standard deviation indicates its precision. The total error is reported as the root mean square error where

$$\text{RSME} = (\sigma^2 + \text{bias}^2)^{1/2}/\gamma_1^{\infty} \times 100\% \tag{28}$$

The purpose of these tests is to design the best experimental method, i.e. the method which minimizes both the

Table 1. Monte Carlo Simulation Results

test no.	exp errors	z	canonical γ_1^∞	canonical γ_2^∞	extrapol curve	eq	mode	av γ_1^∞	std dev	bias	RMSE (%)
1	standard	0.001−0.01	10	5.447	P_D/x_1x_2	1	flash	9.97	0.65	−0.03	6.5
2	standard	0.001−0.01	10	5.447	P_D/x_1x_2	9	flash	9.98	0.65	−0.03	6.5
3	standard	0.001−0.01	10	5.447	x_1x_2/P_D	1	flash	10.52	0.86	+0.52	10
4	$\sigma_P \times 0.5$	0.001−0.01	10	5.447	P_D/x_1x_2	1	flash	9.98	0.34	−0.02	3.4
5	$\sigma_P \times 2$	0.001−0.01	10	5.447	P_D/x_1x_2	1	flash	9.97	1.28	−0.03	12.8
6	$\sigma_T \times 0.5$	0.001−0.01	10	5.447	P_D/x_1x_2	1	flash	9.97	0.65	−0.03	6.5
7	$\sigma_T \times 2$	0.001−0.01	10	5.447	P_D/x_1x_2	1	flash	9.97	0.65	−0.03	6.5
8	$\sigma_h \times 0.5$	0.001−0.01	10	5.447	P_D/x_1x_2	1	flash	9.97	0.64	−0.03	6.4
9	$\sigma_h \times 2$	0.001−0.01	10	5.447	P_D/x_1x_2	1	flash	9.97	0.65	−0.03	6.5
10	standard	0.001−0.01	10	5.447	P_D/x_1x_2	1	recon	9.98	0.57	−0.02	5.7
11	standard	0.022−0.01	10	5.447	P_D/x_1x_2	1	flash	9.91	0.31	−0.09	3.2
12	standard	0.043−0.01	10	5.447	P_D/x_1x_2	1	flash	9.75	0.17	−0.25	3.2
13	standard	0.001−0.01	10	2	P_D/x_1x_2	1	flash	9.92	0.65	−0.08	6.5
14	standard	0.001−0.01	10	10	P_D/x_1x_2	1	flash	9.98	0.65	−0.02	6.5
15	standard	0.001−0.01	100[a]	100	P_D/x_1x_2	1	flash	99.6	1.3	−0.4	1.4
16	standard	0.001−0.01	100[a]	100	x_1x_2/P_D	1	flash	100.4	1.6	+0.4	1.6
17	standard	0.0005−0.005	100[a]	100	P_D/x_1x_2	1	flash	99.8	2.0	−0.2	2.0
18	standard	0.0001−0.001	1000[b]	1000	P_D/x_1x_2	1	flash	988	54	−12	5.5
19	standard	0.0001−0.001	1000[b]	1000	x_1x_2/P_D	1	flash	1010	56	+10	5.7
20	standard	0.00004−0.0004	2500[c]	2500	P_D/x_1x_2	1	flash	2350	460	−150	19
21	$\sigma_P \times 0.1$	0.00004−0.0004	2500[c]	2500	P_D/x_1x_2	1	flash	2350	460	−150	19
22	σ_P, $\sigma_h \times 0.1$	0.00004−0.0004	2500[c]	2500	P_D/x_1x_2	1	flash	2500	80	0	3.1

[a] For $\gamma_1^\infty = \gamma_2^\infty = 100$, $x_1^{sat} = 0.013$ (UNIQUAC calculation). [b] For $\gamma_1^\infty = \gamma^\infty = 1000$, $x_1^{sat} = 0.0010$ (UNIQUAC calculation). [c] For $\gamma_1^\infty = \gamma_2^\infty = 2500$, $x_1^{sat} = 0.000\,40$ (UNIQUAC calculation).

bias and the standard deviation.

Following Hartwick and Howat (1995), the system chosen for most of the tests was acetone + water, and experimental errors were consistent with the original, unmodified equipment. For the last tests (15−22), the acetone + water pure component properties were retained, but the canonical infinite dilution activity coefficients were adjusted to simulate systems which exhibit greater liquid-phase nonideality. All tests were conducted at 315 K. The test parameters correspond to the table columns—experimental errors, bulk composition range (z), canonical infinite dilution activity coefficients γ_1^∞ and γ_2^∞, extrapolation curve (P_D/x_1x_2 or x_1x_2/P_D), use of eqs 1 or 9, and flash or reconciled flash for x_1.

What is the Effect of Using the Rigorous Eq 9 Rather Than the Approximate Eq 1 To Calculate γ_1^∞? Tests 1 and 2 show the results of two sets of simulations. They are identical in all aspects except test 2 includes vapor nonideality. The results show that there is no significant difference between the two results. This is not surprising, since at the canonical temperature, all pressures were below 100 kPa.

For a Given System, Does Extrapolation of P_D/x_1x_2 ***or of*** x_1x_2/P_D ***Minimize the Bias in the Calculation of*** γ_1^∞**?** Tests 1 and 3 show that P_D/x_1x_2 performs somewhat better than x_1x_2/P_D in terms of minimizing random error and substantially better in terms of minimizing bias for the acetone + water system. For the more highly nonideal systems shown in test pairs 15, 16 and 18, 19 there is no significant difference in performance.

What is the Relative Impact of the Various Experimental Errors upon the Precision of the Calculated γ_1^∞? Comparison of tests 4 through 9 to test 1 shows the impact of measurement error on the results. The test 1 errors are those reported by Hartwick and Howat (1995). In the following tests the simulated measurement errors have been adjusted. The precision of the result reflects its sensitivity to measurement error. The accuracy is unaffected. In test 4, the pressure error has been halved, and the standard deviation drops from 0.65 to 0.34. In test 5, the pressure error is doubled, and the standard deviation increases from 0.65 to 1.28. In tests 6 through 9 the temperature and height (metering) errors have been halved and doubled, with no significant effect upon the precision of the results. Figure 4 shows these results graphically. For this level of nonideality and the Hartwick and Howat (1995) error levels, the pressure error is the dominant contributor to the imprecision in γ_1^∞.

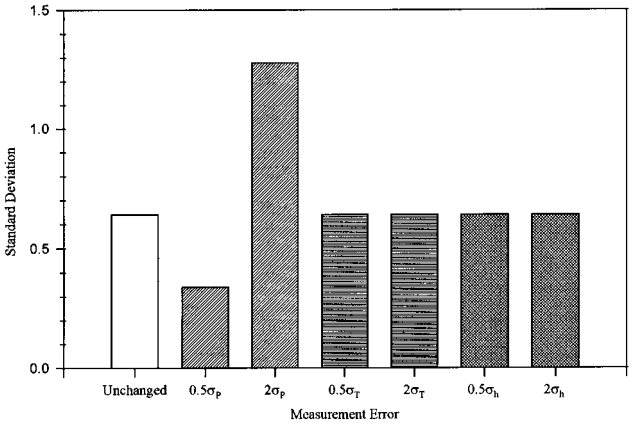

Figure 4. Sensitivity of results to measurement error.

Can Data Reconciliation Techniques Be Used To Minimize the Impact of Experimental Error and Increase the Precision of the Calculated γ_1^∞? When all adjusted variables are used to determine the P,x relationship, the γ_1^∞ algorithm fails to converge, with P,x drifting lower in pressure and greater in liquid mole fraction. Figure 5 shows the P_D/x_1x_2 curve for a series of iterations. Three factors are responsible for this drift and subsequent nonconvergence. First, the flash is overspecified by only one variable. Second, the $P_D/x_1x_2,x_1$ is biased. Third, the pressure error dominates the error in γ_1^∞. These factors combine as follows. First, as indicated by Table 1, the $P_D/x_1x_2,x_1$ description results in a slightly biased estimate for γ_1^∞. This results in slightly low estimates in the activity coefficients used during the next iteration. Because the pressure error is large in the reconciliation and because of the low overspecification, the pressure has less weight compared to the other variables and is preferentially adjusted away from the measured value. The result is that the adjusted pressure is essentially equivalent to that generated by the flash calcula-

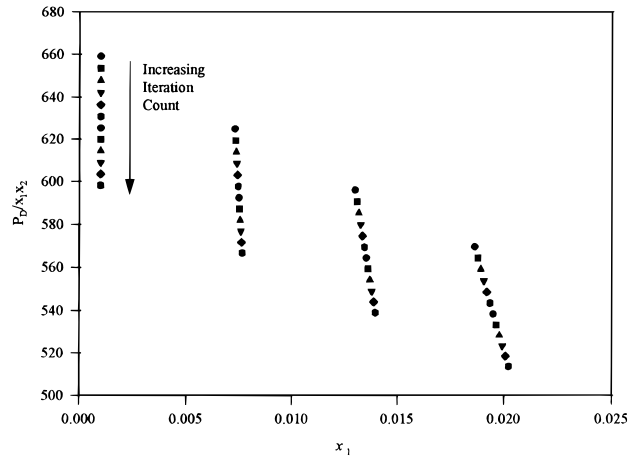

Figure 5. Nonconvergent iterations using all reconciled variables (symbols indicate iteration).

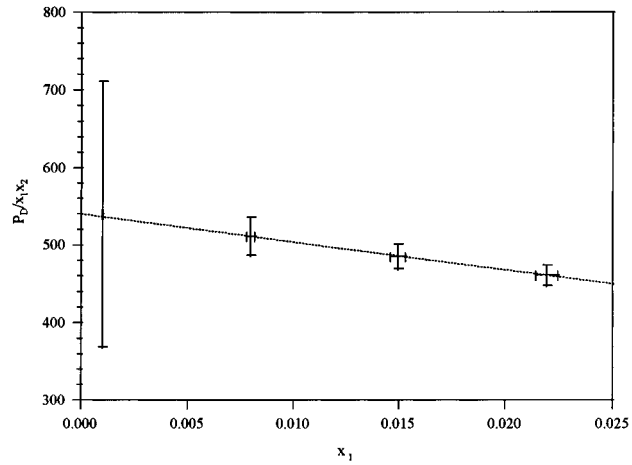

Figure 6. Error for canonical data.

tion. Thus, the bias continues into the next iteration, resulting in further bias.

A modification was incorporated such that reconciliation was used to estimate only the liquid mole fraction. Experimental values for the other variables were used in the development of the $P_D/x_1x_2,x_1$ description. Comparison of test 10 to test 1 shows the effect of this strategy. The bias is not significantly affected. The standard deviation is marginally, but not statistically significantly, improved.

The overall recommendation is that the marginal improvement in precision is not worth the greatly increased complexity and calculation time required for the reconciled flash at these conditions. However, the reconciliation can be further improved by a 'coupled' analysis where the reconciled estimates of the variables, parameters and $P_D/x_1x_2,x_1$ description are determined simultaneously.

For Highly Nonideal Systems Where Two Liquid Phases Can Occur, What Is the Lowest x^{sat} below Which P,x Estimates Are Accurate Enough To Support Reliable Calculation of γ_1^∞? The first step in addressing this question was to run a series of tests to determine the optimal composition range for the system. Comparison of tests 11 and 12 to test 1 shows the effect of raising the upper composition limit. In test 11 the upper composition limit was raised from 0.01 to 0.022. The resulting random error was reduced from 0.65 to 0.31, the bias was increased from −0.03 to −0.09, and the RMSE was decreased from 6.5% to 3.2%. In test 12 the upper composition limit was raised to 0.043. The resulting random error was reduced to 0.17, the bias was increased to −0.25, and the RMSE was 3.2%. Figure 6 is a plot of the canonical data set with error bars for test 11. Note that as the composition increases, the P_D/x_1x_2 error decreases, resulting in lower random error for the intercept and consequently γ_1^∞. However, the nonlinearity of $P_D/x_1x_2,x_1$ and, consequently, the bias of the intercept and γ_1^∞ increase. The optimum lies in using the highest composition limit which does not introduce significant bias. This limit is near 0.022 for acetone + water. For systems in which two liquid phases occur, the upper composition limit should be just below x_1^{sat} to reduce random error subject to limited bias.

The second step was to test the effect of asymmetry. In tests 13 and 14, the canonical value for γ_2^∞ was adjusted. The impact is negligible. Consequently, the value of γ_2^∞ does not impact upon the experimental design analysis, allowing focus on symmetric systems for the third step of this analysis.

The third step was to run a series of tests for symmetric systems which are sufficiently nonideal for two liquid phases to occur. The footnotes below Table 1 give the calculated x_1^{sat}. In tests 15 and 17 two composition ranges were compared for a system with $\gamma_1^\infty = \gamma_2^\infty = 100$. In test 15, the composition range was just below the saturation limit, and in test 17 it was about half the saturation limit. The higher test 15 composition range gave better results. The random error was somewhat lower (1.3 as opposed to 2.0) while the impact of the higher composition on the bias was negligible. Tests 15 and 17 indicate that, for systems which exhibit liquid−liquid behavior, the upper composition for the P_D/x_1x_2 data should be just below x_1^{sat}.

The overall RMSE for test 15 was 1.4%. This is significantly lower than the 6.4% RMSE for the test 14 system ($\gamma_1^\infty = \gamma_2^\infty = 10$) over the same composition range. The shape of the *P,x* curve explains the greater precision of the results for the less ideal system. For a higher γ_1^∞, the slope of the *P,x* curve near infinite dilution is greater. Therefore, the difference between *P* and P°_2 can be measured with greater precision.

As γ_1^∞ increases, the upper composition limit decreases. At some value of x_1^{sat}, the equipment cannot provide precise enough metering in the required range to support independent analysis of γ_1. Test 18 simulates a system with $\gamma_1^\infty = \gamma_2^\infty = 1000$ and $x_1^{sat} = 0.0010$. There is little bias and the random error is 54, giving an RMSE of 5.5%. Test 20 simulates a system with $\gamma_1^\infty = \gamma_2^\infty = 2500$ and $x_1^{sat} = 0.000\,40$. The random error has become intolerably high and there is significant bias. Region 1 analysis has become inadequate.

Test 21 again simulates $\gamma_1^\infty = \gamma_2^\infty = 2500$, but with the pressure error reduced by a factor of 10. There is no improvement, indicating that for this highly nonideal system, pressure error no longer controls the precision of the results. In test 22, the metering error has also been decreased by a factor of 10. The result is substantially better with no bias and a far lower random error. With the higher metering precision, region 1 analysis is appropriate.

Two points are worth noting. First, the appropriate analysis required to determine γ_1^∞ depends upon the precision of the measurements as well as the chemical system. Second, the relative contributions of the errors in the measurements to the error in the estimate for γ_1^∞ vary with the nonideality of the VOC system with pressure error controlling for relatively ideal systems, and metering error controlling for nonideal systems.

Region 1 Experimental Verification

Hartwick and Howat (1995) present experimental measurements and analysis for the acetone + water system at

Table 2. Experimental Data and Calculated Flash Pressure

exptl measurements					flash calculations	
temp (K)	vol (mm^3)	molecular mass of acetone (g/mol × 10^{-3})	molecular mass of water (g/mol)	pressure (kPa)	pressure (kPa)	acetone $10^3\,x$
317.75	9958.48	0.1304	0.248 56	9.57	9.72	0.522
317.73	9958.48	0.4144	0.248 56	10.27	10.35	1.657
317.73	9958.48	0.4414	0.248 56	10.23	10.35	1.657
317.70	9958.48	0.4144	0.248 56	10.20	10.34	1.657
317.72	9958.48	1.3175	0.248 56	12.27	12.30	5.249
317.69	9958.48	1.3176	0.248 56	12.25	12.28	5.250
317.71	9958.48	2.5942	0.248 56	14.62	14.86	10.287
317.75	9958.48	3.8896	0.248 56	17.16	17.28	15.348
317.75	9958.48	0.1341	0.246 70	9.97	9.74	0.541
317.75	9958.48	0.4135	0.246 70	10.72	10.37	1.666
317.73	9958.48	0.4136	0.246 71	10.69	10.36	1.666
317.75	9958.48	1.3277	0.246 70	12.77	12.36	5.329
317.74	9958.48	2.5886	0.246 71	15.41	14.91	10.340
317.74	9958.48	3.8871	0.246 71	18.20	17.32	15.451
317.79	9958.48	0.1271	0.265 43	9.57	9.72	0.477
317.78	9958.48	0.4206	0.265 43	10.36	10.33	1.575
317.81	9958.48	1.3359	0.265 42	12.21	12.22	4.988
317.79	9958.48	2.6005	0.265 43	14.69	14.61	9.667
317.77	9958.48	3.8874	0.265 43	17.04	16.86	14.385
317.76	9958.48	0.4082	0.245 02	10.55	10.37	1.655
317.77	9958.48	1.3285	0.245 01	12.65	12.39	5.369
317.78	9958.48	2.5935	0.245 01	15.28	14.98	10.430
317.75	9958.48	3.9238	0.245 02	17.87	17.44	15.700
333.35	9958.48	1.1817	0.240 07	25.94	26.45	4.847
333.33	9958.48	1.1817	0.240 07	25.96	26.42	4.847
333.35	9958.48	1.9855	0.240 07	29.56	30.41	8.121
333.34	9958.48	2.4812	0.240 07	31.56	32.73	10.131
333.11	9958.48	1.3279	0.232 00	26.37	27.14	5.629
333.09	9958.48	1.3279	0.232 01	26.52	27.11	5.629
333.09	9958.48	1.3279	0.232 01	26.60	27.11	5.629
333.09	9958.48	1.9357	0.232 01	29.28	30.16	8.187
333.08	9958.48	1.9357	0.232 01	29.28	30.15	8.187
333.08	9958.48	2.5580	0.232 01	31.66	33.13	10.795
333.08	9958.48	2.5580	0.232 01	31.72	33.13	10.795
333.08	9958.48	2.5580	0.232 01	31.81	33.13	10.795
333.06	9958.48	2.5581	0.232 01	31.94	33.10	10.795
333.12	9958.48	1.4808	0.228 62	27.33	28.04	6.364
333.11	9958.48	2.2021	0.228 62	30.33	31.64	9.439
333.10	9958.48	2.5181	0.228 62	31.09	33.14	10.781

317 K. Additional acetone + water data at 317 K and 333 K from Hartwick (1996) are presented herein. Table 2 summarizes the experimental measurements and the pressures and mole fractions calculated from the flash for each point.

The 317 K measurements include those reported in Hartwick and Howat (1995) along with new measurements. Analysis using the method established in the experimental design section gives $\gamma_1^\infty = 8.7 \pm 0.3$. The precision of this result is consistent with the precision predicted by the experimental design work over the same composition range. Figure 7 presents the 317 K results as weighted residuals. All weighted residuals should fall between ±2 and should be randomly distributed around zero. The expected value of the sum of the squares of the weighted residuals should be 1. The residuals are random with respect to composition, indicating that the $P_D/x_1x_2,x_1$ curve describes the data equally well along the composition range. There is bias between replicates but less than the expected error. The likely cause is metering errors propagated through each subsequent metering for a replicate set.

Figure 8 shows the difference between the calculated and experimental pressures for the 317 K data. Although the calculated pressures tend to fall above the experimental pressures, there is no trend in composition. There is again bias among replicates. Bear in mind that liquid and bulk compositions are nearly equivalent for this system, so the effect of this difference in calculated and experimental pressure is negligible even though the difference is greater than the anticipated pressure error of 0.1 kPa.

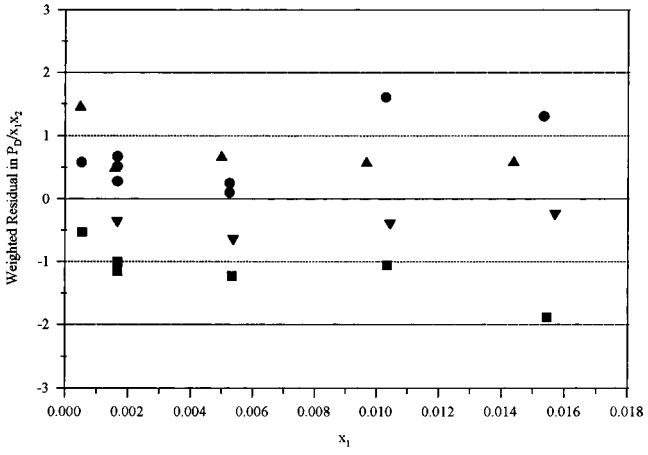

Figure 7. Acetone−water pressure vs composition data at 317 K, weighted residuals.

Table 3 presents a comparison of the 317 K results with literature values. Our value is consistent with the values reported by Hofstee et al. (1960) and Lee (1983) but not with the value reported by Shaw and Anderson (1983).

Analysis of the 333 K data gives $\gamma_1^\infty = 11.8 \pm 0.3$. Figure 9 shows the weighted residuals. As with the 317 K data, the residuals show bias among replicates. All but one point fall between ±2. Figure 10 shows the difference between the calculated and experimental pressures for the 333 K data. The calculated pressures fall below the experimental pressures with a well-defined composition trend.

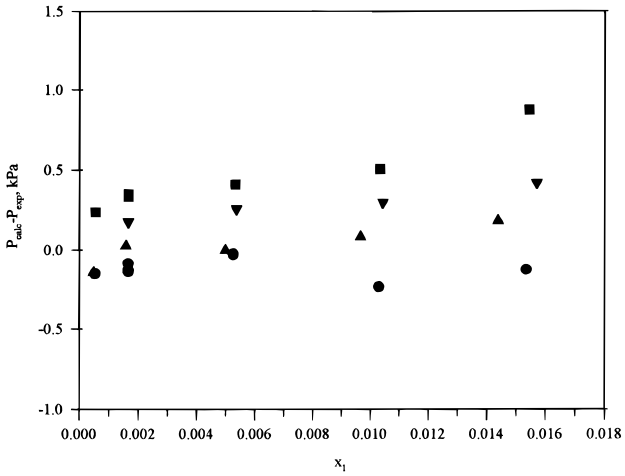

Figure 8. Difference between experimental and calculated pressures at 317 K (symbols indicate replicate measurements).

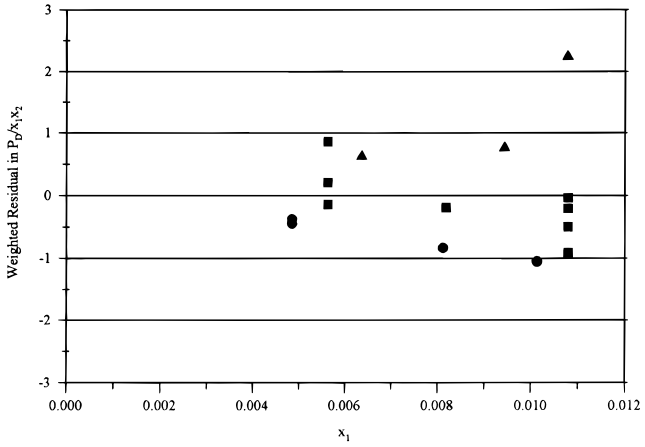

Figure 9. Acetone−water pressure vs composition data at 333 K, weighted residuals.

Table 3. Comparison of Results to Literature Values near 317 K

temp (K)	γ_1^∞	source
317.75	8.7 ± 0.3	this work
313.15	8.20	Shaw and Anderson (1983)
313.15	8.90	Hofstee et al. (1960)
318.15	8.99	Lee (1983)

Table 4. Comparison of Results to Literature Values near 333 K

temp (K)	γ_1^∞	source
333.15	11.8 ± 0.3	this work
333.15	10.8	Hofstee et al. (1960)

Because such trends did not appear for the 317 K data, the 333 K data must be suspect. The transducer was connected directly to cell 6 with transducer held above 333 K, a temperature near the operating limit. The trends shown in Figure 10 result from high-temperature transducer operation. This problem is solved in the Figure 3 system.

Table 4 presents a comparison to literature values. Agreement is only approximate. Additional measurements with the revised equipment configuration are required.

Regions 2 and 3 Experimental Design Results

Table 5 summarizes the experimental design results comparing regions 1, 2, and 3 analysis methods for simulated systems with $\gamma_1^\infty = \gamma_2^\infty = 1000$, 5000, and 10 000. For this set of tests, the errors were consistent with the upgraded experimental equipment, cyclohexane + water

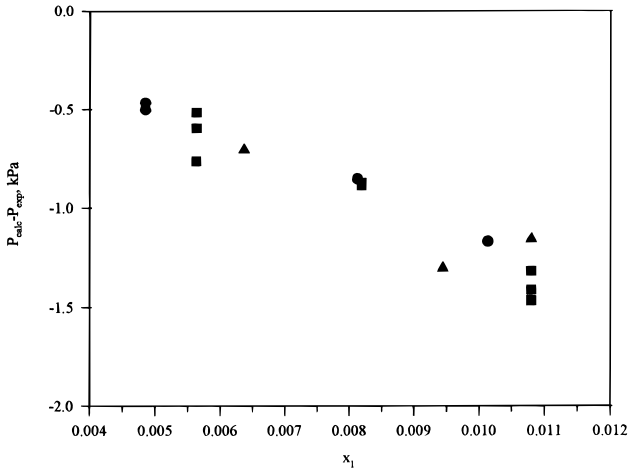

Figure 10. Difference between experimental and calculated pressures at 333 K (symbols indicate replicate measurements).

pure component parameters were used, vapor phase ideality was assumed, the P_D/x_1x_2 curve was used, and 500 Monte Carlo simulations were run for each test. To examine the bias introduced by forcing the solution model to simultaneously calculate vapor−liquid and liquid−liquid−vapor equilibrium, for most of the tests, TK-Wilson was used as the canonical model and UNIQUAC was used as the analysis model.

Tests 1 and 2 show that the region 1 analysis method introduces little bias. However, for $\gamma_1^\infty = \gamma_2^\infty = 5000$, the standard deviation resulting from the error introduced by metering in the small LV region, has become unacceptably high.

Tests 3−5 show that, relative to region 1 analysis, region 2 analysis decreases the standard deviation while increasing bias. This is to be expected, because the region 2 objective function increases reliance on the solution model. For $\gamma_1^\infty = \gamma_2^\infty = 1000$, the increase in bias is unacceptable and region 1 analysis is preferred, but for $\gamma_1^\infty = \gamma_2^\infty = 5000$, the region 2 bias is significantly smaller than the standard deviation and region 2 analysis is preferred.

Tests 6 and 7 show the same trend for region 3 analysis relative to region 2 analysis. Because bulk mole fraction depends on the solution model, region 3 bias is increased, but because relatively large quantities of the saturated liquid are metered, metering error, and consequently standard deviation, are decreased. For $\gamma_1^\infty = \gamma_2^\infty = 5000$, the decrease in random error for region 3 analysis does not compensate for the increase in bias and region 2 analysis is preferred. For $\gamma_1^\infty = \gamma_2^\infty = 10\,000$, the region 3 bias is approximately the size of the standard deviation, but the decrease in standard deviation relative to region 2 analysis is substantial, and region 3 analysis is preferred.

The purpose of tests 8 and 9 was to demonstrate that region 3 solution model dependence is responsible for the bias seen in tests 6 and 7. In tests 8 and 9 UNIQUAC was used as both the canonical and analysis model, and the bias is insignificant.

Conclusions

Three regions in the composition−activity coefficient space have been identified for VOC + water systems which exhibit limited miscibility. The borders between regions depend upon the system nonideality, the experimental equipment limitations and the experimental error. Experimental design simulations suggest that the experimental errors dominating the uncertainty in the activity coefficient estimate vary with system nonideality. Pressure

Table 5. Monte Carlo Simulation Results for Comparison of Region 1, 2, and 3 Analysis Methods

test no.	canonical model	analysis model	region	canonical $\gamma_1^\infty = \gamma_2^\infty$	av γ_1^∞	std dev	bias	RMSE (%)	av x_1^{sat}	std dev	bias	RMSE (%)
1	TK-Wilson	UNIQUAC	1	1000	998	36	−2	3.6	1.052×10^{-3}	0.002×10^{-3}	-0.003×10^{-3}	0.9
2	TK-Wilson	UNIQUAC	1	5000	5010	990	10	19.6	2.061×10^{-4}	0.160×10^{-4}	-0.005×10^{-4}	7.7
3	TK-Wilson	UNIQUAC	2	1000	987	8	−13	1.6	1.054×10^{-3}	0.012×10^{-3}	-0.001×10^{-3}	1.5
4	TK-Wilson	UNIQUAC	2	5000	4950	250	−50	5.2	2.066×10^{-4}	0.115×10^{-4}	0.000×10^{-4}	5.6
5	TK-Wilson	UNIQUAC	2	10,000	10,400	2100	400	20	1.011×10^{-4}	0.122×10^{-4}	0.008×10^{-4}	12
6	TK-Wilson	UNIQUAC	3	5000	4860	120	−140	3.8	2.076×10^{-4}	0.075×10^{-4}	0.010×10^{-4}	3.6
7	TK-Wilson	UNIQUAC	3	10,000	9710	270	−290	4.1	1.033×10^{-4}	0.050×10^{-4}	-0.027×10^{-4}	5.5
8	UNIQUAC	UNIQUAC	3	5000	5000	120	0	2.4	2.023×10^{-4}	0.073×10^{-4}	0.003×10^{-4}	3.6
9	UNIQUAC	UNIQUAC	3	10,000	9990	280	−10	2.8	1.009×10^{-4}	0.050×10^{-4}	0.003×10^{-4}	5.0

errors dominate for nearly ideal systems and metering errors dominate for highly nonideal systems.

A data analysis procedure incorporating data reconciliation and all experimental errors has been analyzed. Decoupled implementation is unworkable due to bias in the extrapolation in the excess pressure function. A limited implementation using reconciliation only to estimate liquid mole fractions provides no significant improvement in the estimated activity coefficient. A coupled reconciliation−activity coefficient estimation should be developed to improve the precision in the activity coefficient estimate.

Data for the acetone−water binary at 317 K and 333 K are reported. The description of the data is within experimental error; however, there is bias among the replicates. The most notable cause is the potential uncertainty in the pressure measurement due to the transducer temperature control. Experimentalists using a Paroscientific transducer should operate it near room temperature, taking extreme care to ensure that liquid does not form in the transducer.

Compared to region 1 analysis applied to systems having limited miscibility, the application of region 2 analysis decreases random error and increases the potential for bias caused by solution model dependence. Applying region 3 analysis to highly nonideal systems further reduces the random error but increases the solution model induced bias.

Acknowledgment

A very special thanks to Dr. G. W. Swift, Distinguished Professor Emeritus, for his unselfish advice, guidance, and friendship.

Nomenclature

A, B, C, D	Miller vapor pressure equation coefficients
bias	statistical bias between estimated and canonical value
F	moles of chemical metered into test cell
$\vec{f}$	vector of constraints
J	variance−covariance matrix
l	eqs A-2
P	total pressure
P°	vapor pressure
q	UNIQUAC pure component parameter
r	UNIQUAC pure component parameter
PC	Poynting correction
Q	constrained objective function
Q	matrix of partial derivatives
R	gas constant
RSME	root mean square error
S	objective function value (eq 13)
T	temperature
$u_{ji} - u_{ii}$	binary interaction parameter used in UNIQUAC solution model
*V**	characteristic volume used in liquid molar volume correlation, liters/mole
v	liquid molar volume
VOC	volatile organic chemical
x	liquid-phase composition (mole fraction)
y	vapor-phase composition (mole fraction)
$\vec{Z}$	vector of variables
$\Delta\vec{Z}$	vector of differences between adjusted and measured variables
z	overall composition (mole fraction)
γ	activity coefficient
$\vec{\lambda}$	vector of Lagrange multipliers
θ	eqs A-2
$\vec{\theta}$	vector of parameters
Φ	eqs A-2, grouped nonidealities
ϕ	fugacity coefficient
σ	standard deviation
τ	interaction parameter in UNIQUAC model, eqs A-2
ω_{SRK}	acentric factor used in liquid molar volume correlation

Subscripts

c	value at the critical point
D	departure
i	component in a mixture, general
j	component in mixture, general
z	derivatives with respect to variables
θ	derivatives with respect to parameters
λ	derivatives with respect to Lagrange multipliers
k	component in mixture, general
1	component 1 of a mixture, VOC
2	component 2 of a mixture, water
°	"true" value of a parameter

Superscripts

C	combinatorial contribution to activity coefficient, eqs A-2.
id	ideal
L	liquid
R	residual contribution to activity coefficient, eqs A-2.
T	transpose
V	vapor
sat	liquid saturation limit
*	second liquid phase
−	partial molal quantity
−1	inverse
^	mixture property
°	pure component property
∞	at infinite dilution conditions

Appendix

This section presents the supporting equations for vapor pressure, activity coefficient, and molar volume. Values for the acetone and water physical property parameters required by these equations and used in the experimental data analysis are also reported.

Supporting Equations

Vapor Pressure (Miller, 1964)

$$P_i^{\circ}/\mathrm{kPa} = \exp(A_i/(T/\mathrm{K}) + B_i + C_i(T/\mathrm{K}) + D_i(T/\mathrm{K})^2) \quad \text{(A-1)}$$

UNIQUAC Solution Model

(Abrams and Prausnitz, 1975)

$$\ln \gamma_i = \ln \gamma_i^{\mathrm{C}} + \ln \gamma_i^{\mathrm{R}} \quad \text{(A-2a)}$$

$$\ln \gamma_i^{\mathrm{C}} = \ln \frac{\Phi_i}{x_i} + \frac{z}{2} q_i \ln \frac{\theta_i}{\Phi_i} + l_i - \frac{\Phi_i}{x_i} \sum_j x_j l_j \quad \text{(A-2b)}$$

$$\ln \gamma_i^{\mathrm{R}} = -q_i \ln\left(\sum_j \theta_j \tau_{ji}\right) + q_i - q_i \sum_j \frac{\theta_j \tau_{ij}}{\sum_k \theta_k \tau_{kj}} \quad \text{(A-2c)}$$

$$l_j = \left(\frac{z}{2}\right)(r_j - q_j) - (r_j - 1) \quad \text{(A-2d)}$$

$$\theta_i = \frac{q_i x_i}{\sum_j q_j x_j} \quad \text{(A-2e)}$$

$$\Phi_i = \frac{r_i x_i}{\sum_j r_j x_j} \quad \text{(A-2f)}$$

$$\tau_{ji} = \exp\left(-\frac{u_{ji} - u_{ii}}{RT}\right) \quad \text{(A-2g)}$$

and note that $\tau_{ii} = \tau_{jj} = 1$.

Liquid Density (Hankinson and Thomson, 1979)

$$V^{\mathrm{L}} = V^*(V_r^{(0)}(1 - \omega V_r^{(\delta)})) \quad \text{(A-3a)}$$

$$V_r^{(0)} = 1 - 1.52816(1 - T_r)^{1/3} + 1.43907(1 - T_r)^{2/3} - 0.81446(1 - T_r) + 0.190454(1 - T_r)^{4/3} \quad \text{(A-3b)}$$

$$V_r^{(\delta)} = (-0.296123 + 0.386914T_r - 0.0427258T_r^{\,2} - 0.0480645T_r^{\,3})/(T_r - 1.00001) \quad \text{(A-3c)}$$

Physical Property Parameters

Table A-1. Pure Component Properties and Correlation Coefficients

	acetone (1)	water (2)
Vapor Pressure Coefficients (Eq A-1)		
A	−4958.529	−6267.821
B	25.5409	26.4272
C	-2.40254×10^{-2}	-1.75385×10^{-2}
D	1.89008×10^{-5}	1.10070×10^{-5}
Liquid Density Correlation		
$V^*/\mathrm{m^3 \cdot mol^{-1}}$	2.080×10^{-4}	4.35669×10^{-5}
ω_{SRK}	0.3149	−0.65445
T_c (specific to correlation)/K	508.15	647.37
T_c/K	508.1	647.3
P_c/kPa	4701	22120
mol wt	58.080	18.015
Solution Model Canonical Parameters		
$u_{ji} - u_{ii}/\mathrm{kJ \cdot mol^{-1}}$	3.166	−0.5773
q	2.336	1.400
r	2.5735	0.920

Literature Cited

Abrams, D. S.; Prausnitz, J. M. Statistical Thermodynamics of Liquid Mixtures: A New Expression for the Excess Gibbs Energy of Partly or Completely Miscible Systems. *AIChE J.* **1975**, *21* (1), 116−128.

Britt, H. I.; Luecke, R. H. The Estimation of Parameters in Nonlinear Implicit Models. *Technometrics* **1973**, *15* (2), 233−247.

Ellis, S. R. M.; Jonah, D. A. Prediction of Activity Coefficients at Infinite Dilution. *Chem. Eng. Sci.* **1962**, *17*, 971−976.

Gautreaux, M. F., Jr.; Coates, J. Activity Coefficients at Infinite Dilution. *AIChE J.* **1955**, *1* (4), 406−500.

Hankinson, R. W.; Thomson, G. H. A New Correlation for Saturated Densities of Liquids and Their Mixtures. *AIChE J.* **1979**, *25* (4), 653−663.

Hartwick, R. P. Infinite Dilution Activity Coefficients of Acetone in Water: A New Experimental Method and Verification. Masters Thesis, University of Kansas, 1996.

Hartwick, R. P.; Howat, C. S. The Contribution of Phase Equilibria to the Uncertainty in Volatile Organic Chemical Removal from Waste Water Using Distillation. Mid-America AIChE Regional Conference, Kansas State University, Manhattan, Kansas, 1993.

Hartwick, R. P.; Howat, C. S. Infinite Dilution Activity Coefficients of Acetone in Water: A New Experimental Method and Verification. *J. Chem. Eng. Data* **1995**, *40* (4), 738−745.

Hofstee, M. T.; Kwantes, A.; Rijnders, C. W. A. Symposium Distillation Brighton **1960**, *105* (1060) (as found in Tiegs et al. (1986)).

Howat, C. S. Vapor-Liquid Equilibria of the n-Pentane-2-Methyl-1,3-Butadiene System at 100F. Masters Thesis, University of Kansas, 1975.

Kuo, D. Comparison of Separate, Sequential and Simultaneous Methods for Data Reconciliation and Efficiency Estimation for Multiple Flash Configurations. Masters Thesis, University of Kansas, 1988.

Laurance, D. R.; Swift, G. W. Vapor-Liquid Equilibria in Three Binary and Ternary Systems Composed of n-Butane, Butene-1, and Butadiene-1,3. *J. Chem. Eng. Data* **1974**, *19* (1), 61−67.

Lee, H. J. *Hwahak Konghak* **1983**, *21*, 317 (as found in Tiegs et al. (1986)).

MacDonald, R. J.; Howat, C. S. Data Reconciliation and Parameter Estimation in Plant Performance Analysis. *AIChE J.* **1988**, *34* (1), 1−8.

Maher, P. J.; Smith, B. D. Infinite Dilution Activity Coefficient Values from Total Pressure VLE Data. Effect of Equation of State Used. *Ind. Eng. Chem. Fundam.* **1979**, *18* (4), 354−357.

Miller, D. G. Estimating Vapor Pressures. A Comparison of Equations. *Ind. Eng. Chem.* **1964**, *56* (3), 46−57.

Natarajan, S. K. Personal communication, 1995.

Renon, H.; Prausnitz, J. M. Local Compositions in Thermodynamic Excess Functions for Liquid Mixtures. *AIChE J.* **1968**, *14* (1), 135−144.

Shaw, D. A.; Anderson, T. F. Use of Gas Chromatographic Headspace Analysis in Vapor-Liquid Equilibrium Data Collection. *Ind. Eng. Chem. Fundam.* **1983**, *22*, 79−83.

Tiegs, D.; Gmehling, J.; Mediva, A.; Soares, M.; Bastos, J.; Alessi, P.; Kikic, I. *Activity Coefficients at Infinite dilution*. DECHEMA Chemistry Data Series: DECHEMA: Frankfurt, 1986; Vol IX, Parts 1−4.

Tsuboka, T.; Katayama, T. Modified Wilson Equation for Vapor-Liquid and Liquid-Liquid Equilibria. *J. Chem. Eng. Jpn.* **1975**, *8* (3), 181−187.

Walas, S. M. *Phase Equilibria in Chemical Engineering*; Butterworths Publishers: Boston, 1985; 671 pp.

Received for review January 27, 1996. Accepted June 24, 1996.[⊗] The authors acknowledge the generous support of the Occidental Petroleum Foundation which supplied funds for the purchase of equipment and supplies for this project. The authors acknowledge the support of the Department of Chemical & Petroleum Engineering for the partial support of J.N.H.

JE960026Z

[⊗] Abstract published in *Advance ACS Abstracts*, August 1, 1996.